Catal Lett (2015) 145:576–582
DOI 10.1007/s10562-014-1408-0

Oxygen-Nonstoichiometric $YBaCo_4O_{7+\delta}$ as a Catalyst in H_2O_2 Oxidation of Cyclohexene

Outi Parkkima · Ana Silvestre-Albero ·
Joaquin Silvestre-Albero · Maarit Karppinen

Received: 20 September 2014 / Accepted: 21 October 2014 / Published online: 31 October 2014

Abstract Here we present oxygen-nonstoichiometric transition metal oxides as highly prominent candidates to catalyze the industrially important oxidation reactions of hydrocarbons when hydrogen peroxide is employed as an environmentally benign oxidant. The proof-of-concept data are revealed for the complex cobalt oxide, $YBaCo_4O_{7+\delta}$ ($0 < \delta < 1.5$), in the oxidation process of cyclohexene. In the 2-h reaction experiments $YBaCo_4O_{7+\delta}$ was found to be significantly more active (>60 % conversion) than the commercial TiO_2 catalyst (<20 %) even though its surface area was less than one tenth of that of TiO_2. In the 7-h experiments with $YBaCo_4O_{7+\delta}$, 100 % conversion of cyclohexene was achieved. Immersion calorimetry measurements showed that the high catalytic activity may be ascribed to the exceptional ability of $YBaCo_4O_{7+\delta}$ to dissociate H_2O_2 and release active oxygen to the oxidation reaction.

Keywords Nonstoichiometric oxide · Catalyst · Hydrocarbon oxidation · H_2O_2 oxidant

1 Introduction

Catalytic oxidation of alcohols and hydrocarbons is an important industrial process in both environmental chemistry (e.g. removal of VOCs) and fine chemical industry [1–3]. These oxidation processes involve the conversion of the corresponding chemicals into intermediates (e.g. epoxides, alcohols, etc.) and/or into carbon dioxide and water as a final product. In particular—from the economical point of view—partial oxidation of alkenes to produce epoxides is one of the momentous industrial reactions since epoxides are synthetic precursors for numerous fine chemicals and polymer syntheses [4], e.g. production of propylene oxide via epoxidation of propylene using *tert*-butyl hydroperoxide [5]. The epoxide intermediates are catalytically produced from the corresponding alkenes via oxygen transfer reactions using a peroxy acid as an oxidant and a transition metal compound as a catalyst [6, 7]. The role of the active metal in such oxidation reactions is to activate the oxygen–oxygen bond in the peroxo acid (η^2-coordinated peroxide) in order to supply electrophilic oxygen able to react with the alkene molecule [6, 8]. Among the different transition metal catalysts, Ti-based systems have been the most widely investigated. Besides the Shell catalyst based on Ti(IV)-SiO_2, there have been numerous efforts to design variously substituted Ti(IV)-framework materials, e.g. TS-1, Ti-MCM41, etc., with excellent catalytic performance in the aforementioned peroxo-acid oxidized reactions [9–12]. X-ray absorption spectroscopy analysis has revealed that four-coordinated Ti(IV) centers indeed are the active sites for the oxidation reactions [13].

While peroxo acids are by far the most commonly employed oxidants in the epoxidation reactions, there are certain drawbacks commonly associated with their use such as a low reaction rate and the large amounts of these acids typically remaining as an unwanted residue in the product. Hence, alternative strong and green oxidants such as hydrogen peroxide are urgently searched for. Hydrogen peroxide is easy to handle and it yields an environmentally

O. Parkkima · M. Karppinen (✉)
Laboratory of Inorganic Chemistry, Department of Chemistry,
Aalto University, 00076 Aalto, Finland
e-mail: maarit.karppinen@aalto.fi

A. Silvestre-Albero · J. Silvestre-Albero (✉)
Laboratorio de Materiales Avanzados, Departamento de
Química Inorgánica-Instituto Universitario de Materiales,
Universidad de Alicante, Ap. 99, 03080 Alicante, Spain
e-mail: joaquin.silvestre@ua.es

benign by-product, i.e. water. Unfortunately, aqueous H_2O_2 exhibits a poor catalytic performance on Ti(IV) centers supported on mesoporous silica due to the competitive adsorption between H_2O_2 and H_2O on the hydrophilic Ti(IV) sites. Consequently, new catalytic systems are desired which would efficiently decompose H_2O_2 and yield active electrophilic oxygen.

Besides titanium, other transition metals such as cobalt have also been investigated as potential catalysts in the oxidation of alkenes [14–16]. Interestingly, partial substitution of tetrahedrally-coordinated Al(III) and P(V) in aluminophosphates by Co(III) and Ti(IV) resulted in excellent catalysts for the oxidation of olefins when acetyl peroxyborate was used as the oxidant [15]. The redox-active cobalt centers apparently provided the location for the initiation and generation of free-radical intermediates for the catalytic oxidation. Unfortunately, these Co-based catalysts were found inactive when H_2O_2 was used as the oxidant [16].

In recent years several families of oxygen-nonstoichiometric transition metal oxide materials have been intensively investigated—largely due to their intrinsic redox properties—for a variety of modern materials technologies ranging from superconducting, thermo-electric, ferroelectric and magnetic devices to batteries, fuel cells, sensors and oxygen-storage devices. These materials have however remained rather unexplored in catalysis. Cerium oxide is the most widely-used oxygen-storage material; it is also known to be an active catalyst in various reactions [17]. Recently it was also shown to be active in epoxidation reactions [18]. Here our hypothesis is that in addition to ceria, other oxygen-nonstoichiometric and thereby redox-active transition metal oxides would be highly potential material candidates for next-generation catalyst systems involving the catalytic oxidation of hydrocarbons with H_2O_2. As the first candidate material to be investigated we selected the complex cobalt oxide, $YBaCo_4O_{7+\delta}$ ($0 < \delta < 1.5$). It has a significantly larger oxygen-storage capacity (2,600 μmolO/g [19]) than the best ceria derivative CeO_2–ZrO_2 (1,500 μmolO/g [20]). In addition, $YBaCo_4O_{7+\delta}$ releases all the stored oxygen in air at appreciably low temperatures below 400 °C whereas ceria requires a harsh reducing atmosphere and a much higher temperature for the oxygen release. As shown in Fig. 1, the crystal structure of $YBaCo_4O_{7+\delta}$ contains corner-sharing CoO_4 tetrahedra of mixed-valent Co(II/III) [21]. Despite its unique properties—the large low-temperature oxygen mobility, the wide range of oxygen-nonstoichiometry and the presence of tetrahedrally coordinated Co(II/III) centers [19, 22–26]—and the fact that it has already been considered as a promising oxygen buffer in various other applications (for a review, see [27]), the $YBaCo_4O_{7+\delta}$ phase has not yet been exploited in heterogeneous catalysis. Here we will report our highly promising results on the catalytic performance of $YBaCo_4O_{7+\delta}$ in the oxidation of cyclohexene in combination with H_2O_2 as the green oxidant. The performance is discussed in comparison to those of a simple binary cobalt oxide powder and commercial titanium oxide (P25) powder.

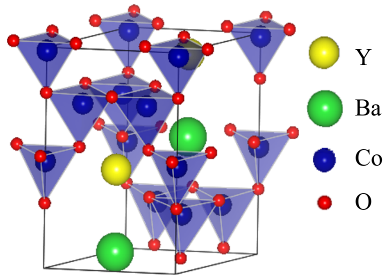

Fig. 1 Schematic illustration of the crystal structure of $YBaCo_4O_{7+\delta}$

2 Experimental

2.1 Catalyst Sample Preparation

The $YBaCo_4O_{7+\delta}$ sample was prepared through a solid state synthesis route from appropriate amounts of the starting material powders, Y_2O_3 (99.9 %), $BaCO_3$ (>99 %) and Co_3O_4 (99.7 %), thoroughly ground with ethanol and calcined in air at 900 °C for 12 h. The calcined sample powder was pressed into a pellet of ~1 g and fired in air at 1,150 °C for 30 h, followed by furnace-cooling down to room temperature. After the synthesis the sample was pulverized, and the oxygen content of the powder was adjusted to $\delta \approx 0$ by annealing it in a tube furnace in an Ar gas flow at 500 °C for 10 h after which the furnace was slowly cooled down.

Additionally a simple binary cobalt oxide sample was prepared for reference by heat-treating 1 g of commercial cobalt oxide (Co_3O_4, 99.7 %, Merck) at 1,150 °C in air for 15 h. For the sake of comparison the catalytic activity of a commercial titanium oxide material (P25, Aldrich) was investigated too.

2.2 Basic Characterization of Sample Powders

Phase purity/composition of the samples was confirmed by X-ray powder diffraction (XRD; Panalytical X́Pert Pro MPD, $CuK_{\alpha1}$ radiation, PixCel detector) measurements. Specific surface area was determined for the sample powders through the BET equation from the N_2 adsorption data obtained at −196 °C using an in-house designed and developed volumetric equipment. Before the adsorption experiments the samples were degassed at 250 °C for 4 h.

The precise oxygen content of the $YBaCo_4O_{7+\delta}$ powder was analyzed by iodometric titration [28]. About 20 mg of finely ground sample powder was dissolved in oxygen-free 1 M HCl in an air-tight cell under constant N_2 gas (99.999 %) bubbling, aided with a significant excess of potassium iodide (ca. 1.5 g). The iodine formed in the redox reaction between trivalent cobalt and iodide was titrated with standard 0.010 M Na_2SO_3 solution (Merck) in the presence of starch indicator. The experiment was repeated three times with an excellent reproducibility. The oxygen content of the cobalt oxide reference powder could not be determined by titration because the material was insoluble in 1 M HCl. For this reason, the precise stoichiometry of our binary cobalt oxide sample was investigated by thermogravimetric (TG; Pyris 1 TGA) reduction. A sample specimen of ca. 20 mg was heated to 800 °C with a heating rate of 5 °C/min in an H_2 (5 %)/Ar gas flow. During this reductive TG run the oxide is reduced to Co metal, and the initial amount of oxygen in the sample can be calculated from the overall weight loss. The same thermobalance was used to confirm the oxygen absorption/desorption characteristics of the $YBaCo_4O_{7.05}$ sample powder in O_2 gas flow. In these experiments a sample specimen of $\sim$20 mg was slowly (1 °C/min) heated from room temperature to 500 °C in an O_2 gas flow (40 ml/min).

The chemical state of the catalyst surface was investigated by X-ray photoelectron spectroscopy (XPS; VG-Microtech Multilab 3000 spectrometer, hemispherical electron analyzer, Mg–K$_\alpha$ ($h = 1{,}253.6$ eV; 1 eV $= 1.6302 \times 10^{-19}$ J) 300-W X-ray source). The sample powder was pressed into a small Inox cylinder and mounted on a sample rod placed in a pretreatment chamber before being transferred to the analysis chamber. Before recording the spectrum, the sample was maintained in the analysis chamber until a residual pressure of ca. 5×10^{-7} N/m^2 was reached. The spectra were collected at pass energy of 50 eV. All binding energies were referenced to the C 1s line at 284.6 eV, which provided binding energy values with an accuracy of ±0.2 eV.

2.3 Catalytic Evaluation

Catalytic studies were performed using cyclohexene (99 %, Aldrich) as the substrate and hydrogen peroxide as the primary oxidant. In a typical reaction, 2 mmol of cyclohexene, 2 mmol of H_2O_2 (30 wt% in water, Aldrich), 40 mg of the catalyst powder, 0.25 ml of octane as an internal standard and 1-propanol as a solvent up to 5.8 ml final volume were added to a 50 ml round-bottom flask fitted with a reflux condenser. The reaction mixture was stirred at 70 °C for 2 h (in some experiments also for a longer period of time). The reaction was terminated by quenching with water. The catalyst was separated by filtration and the reaction products were analyzed by on-line gas-chromatography (Shimadzu GC-2010, flame ionization detector FID) and a capillary column HP-5. Blank experiments were performed using the same experimental conditions without a catalyst.

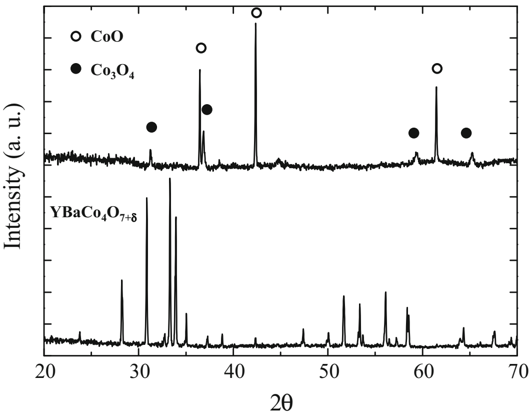

Fig. 2 XRD patterns for the $YBaCo_4O_{7+\delta}$ sample and the cobalt-oxide reference powder

To understand the nature of the catalytic reaction, immersion calorimetry measurements into H_2O_2 (30 wt% in water, Aldrich) were performed in a Setaram Tian-Calvet C80D calorimeter working at 30 °C. Prior to the experiment, the sample specimen was degassed in glass-made vacuum equipment down to 10^{-3} Pa at 250 °C for 4 h. After degassing, the glass bulb containing the sample was sealed into vacuum and inserted into the calorimetric chamber containing the immersion liquid. Once thermal equilibrium is reached, the brittle tip of the glass bulb is broken and the heat of interaction is recorded as a function of time. The total enthalpy of immersion ($-\Delta H_{\mathrm{imm}}$) is obtained by integration of the signal, after appropriate corrections for the breaking of the tip (exothermic) and the heat of evaporation of the immersion liquid necessary to fill the empty volume of the bulb with the vapor at the corresponding vapor pressure (endothermic).

3 Results and Discussion

3.1 Chemical Characteristics of the Catalyst Powders

Figure 2 shows XRD patterns for the two cobalt-oxide powders investigated. The binary cobalt oxide reference sample is a mixture of two phases, CoO as the main phase and Co_3O_4 with a lesser amount [29, 30]. The average oxygen content of the sample was determined to be $CoO_{1.04}$ on the basis of TG analysis. For the $YBaCo_4O_{7+\delta}$ sample, XRD confirms the presence of a single phase. The lattice parameters were readily refined from the XRD

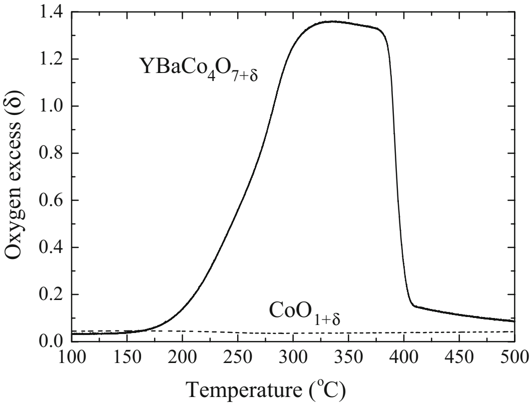

Fig. 3 TG curves for the $YBaCo_4O_{7+\delta}$ sample and the cobalt-oxide reference powder recorded in an O_2 gas flow (heating rate 1 °C/min)

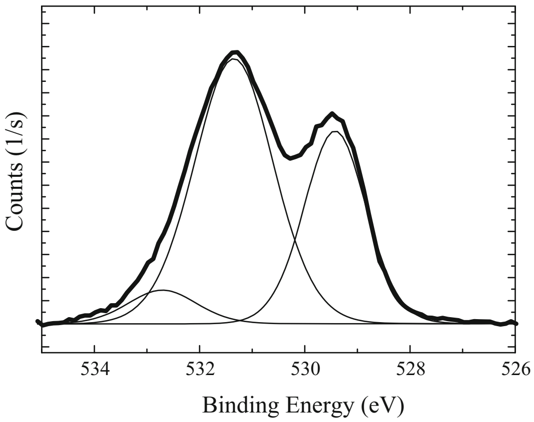

Fig. 4 O 1s core level spectra for $YBaCo_4O_{7.05}$. The measured data are presented with the *thick black line* and the convoluted peaks are presented with thinner lines

pattern in space group $P6_3mc$, with $a = 6.3033$ Å and $c = 10.2414$ Å, as expected from our previous work [19]. Iodometric titration experiments gave the oxygen content for the $YBaCo_4O_{7+\delta}$ sample at $\delta = 0.05$. Hence, in both of our cobalt-oxide samples cobalt exists with a mixed II/III valence.

Figure 3 shows the TG curves recorded for the $YBaCo_4O_{7.05}$ sample and also for the $CoO_{1.04}$ reference upon heating in an O_2 gas flow up to 500 °C. For the reference cobalt oxide no oxygen absorption/desorption is seen in this temperature range. The oxygen content of $YBaCo_4O_{7.05}$ also remains unchanged upon heating up to ca. 200 °C, but above this temperature the material exhibits a sudden weight increase, indicating a substantial increase in the oxygen content up to $\delta \approx 1.4$, followed by a weight/oxygen loss upon further heating around 400 °C. Hence our $YBaCo_4O_{7+\delta}$ sample indeed possesses the remarkable oxygen absorption/desorption or redox capability as expected from previous works [19, 22–27].

The surface area of the $YBaCo_4O_{7.05}$ sample powder was determined by the BET method to be very low ($\sim$2 m^2/g) as the sample was synthesized through solid-state synthesis at the relatively high temperature of 1150 °C. For comparison, the surface area of the commercial TiO_2 reference powder is $\sim$50 m^2/g.

The chemical nature of the surface species in the $YBaCo_4O_{7.05}$ sample was evaluated by XPS; the O 1s core level spectrum is presented in Fig. 4. There are three spectral components found at 529.4 eV (33 % of total O), 531.4 eV (59 %) and 532.7 eV (6.6 %). The pattern corresponds to a typical transition metal oxide surface like that of NiO [31], Cr_2O_3 [32] or Co_3O_4 [33]. Only the first peak at 529.4 eV is probably due to the lattice oxygen. The major peak in the middle has been proposed to be due to defective sites within the crystal, adsorbed oxygen or hydroxide [34]. The smallest peak at the highest energy (which could probably be convoluted into several smaller peaks) is most likely due to traces of organic compounds (alcohols, esters etc.) or adsorbed water [34]. The binding energy values are somewhat lower than those of the binary Co(II,III) oxide Co_3O_4 (530.0–530.8–532.7) [33], which is consistent with the fact that the other cation species (Y and Ba) in this lattice are much more electropositive than cobalt. Corresponding values for lattice O 1s in Y_2O_3 and BaO are 529.0 eV [35] and 528.2 eV [36], respectively. Actually, for mixed oxides containing different metal species somewhat average binding energy values are expected from those for the individual binary oxides [36].

The XPS spectrum for Y 3d was found to have two peaks corresponding to the spin orbital splitting of $3d_{5/2}$ (156.7 eV) and $3d_{3/2}$ (158.7 eV): the binding energy values are similar to those reported for Y(III) [37]. For samples containing both Co and Ba, XPS is not the optimal analysis tool due to the overlap of Co 2p and Ba 3d spectra in the energy range of 770–800 eV [38, 39]. Luckily, from the oxygen content analysis we know that in the $YBaCo_4O_{7.05}$ sample and also in the $CoO_{1.04}$ reference cobalt exists with a mixed II/III valence.

3.2 Catalytic Activity

The catalytic behavior was studied for the two cobalt-oxide powders, $YBaCo_4O_{7.05}$ and $CoO_{1.04}$, in the oxidation process of cyclohexene with the H_2O_2 oxidant. The epoxidation of cyclohexene is a well-known reaction with two different reaction mechanisms, the radical route giving rise to 2-cyclohexen-1-ol and cyclohexene oxide via allylic oxidation through cyclohexenyl hydroperoxide, and the direct oxidation pathway to cyclohexene oxide and 1,2-cyclohexane-diol, after a subsequent ring-opening by

Table 1 Product distribution for the catalytic oxidation of cyclohexene

Sample	Product distribution %				
	Epoxide	Ketone	Ether	Alcohol	Diol
$YBaCo_4O_{7+\delta}$	71.1	5.0	10.9	0	12.9
P25	26.7	1.3	27.1	1.9	42.9
$CoO_{1+\delta}$	0	0	32.2	27.1	40.7

H_2O present in the reaction media. For both the cobalt-oxide catalysts, the main reaction products were 2-cyclohexen-1-ol (alcohol), 2-cyclohexene-1-one (ketone), 1,2-cyclohexane-diol (diol) and its corresponding mono ether (ether), and cyclohexene oxide (epoxide), although the relative amounts of these components somewhat varied depending on the catalyst material and the catalytic conditions (reaction temperature and time). In Table 1, we summarize the composition of the reaction product for selected representative experiments.

The product distribution obtained for the different catalysts evaluated in the oxidation of cyclohexene suggests that the direct epoxidation mechanism must prevail over the radical mechanism, except for the $CoO_{1+\delta}$ catalyst where the large proportion of 2-cyclohexen-1-ol suggests some contribution from the radical mechanism. Concerning the selectivity to the most valuable reaction product, the epoxide, $YBaCo_4O_{7+\delta}$ catalyst exhibits an exceptional behavior with a selectivity value as high as 71 %. This selectivity achieved using 1-propanol as a solvent and H_2O_2 as an oxidant highly overpasses the selectivity for the reference sample, P25, with a value around 25 % and that of $CoO_{1+\delta}$ with a value close to 0. The poor selectivity of the last two catalysts must be attributed to their high ability to hydrolyze the epoxide into the diol (high selectivity to 1,2-cyclohexane-diol), a process assisted by H_2O introduced into the reaction media by aqueous 30 % H_2O_2 solution and the decomposition of H_2O_2. Apparently, allylic oxidation and ring-opening of the epoxide, the two major side reactions in the epoxidation of cyclohexene that are responsible for the low selectivity to the epoxide, are inhibited in the presence of the $YBaCo_4O_{7+\delta}$ catalyst.

To evaluate the catalytic performance of the different catalysts, Fig. 5a compares the catalytic conversion for the cyclohexene oxidation at 70 °C after a reaction time of 2 h. As it can be observed, not only the conventional transition-metal catalyst TiO_2 but also the binary cobalt-oxide $CoO_{1.04}$ exhibit a poor catalytic conversion efficiency (not much enhanced compared to the blank experiment). This is most likely due to the difficulties of these systems to activate/dissociate the O–O bond in H_2O_2, like also observed earlier with similar binary oxides [16]. Quite remarkably, for our complex cobalt oxide, $YBaCo_4O_{7+\delta}$, a nearly three-fold increase in the catalytic conversion efficiency from 20 % to nearly 60 % was achieved. Moreover, as it can be observed in Fig. 5b, completely conversion of cyclohexene was achieved for $YBaCo_4O_{7+\delta}$ in 7 h. From these results it can be envisaged that $YBaCo_4O_{7+\delta}$ is an extraordinarily active catalyst for cyclohexene oxidation, and apparently even when H_2O_2 is used as the oxidant, with comparable values in terms of conversion and selectivity towards the epoxide to the best catalysts reported in the literature for transition metal based catalysts [40–42].

To further confirm the exceptional behavior of $YBaCo_4O_{7+\delta}$ as an oxidation catalyst, and more specifically in the activation of the H_2O_2 molecule, immersion calorimetry measurements were performed. Immersion calorimetry is a powerful technique to estimate the enthalpy of immersion of a liquid molecule on a solid surface; it depends on the surface area available to the liquid, the porosity of the solid and the specific interactions of the liquid molecule with the solid surface [43]. Taking into account that in heterogeneous catalysis the degree of the interaction between the reactants and the active sites determines the catalytic behavior, e.g. the activation of the oxidant [44], immersion

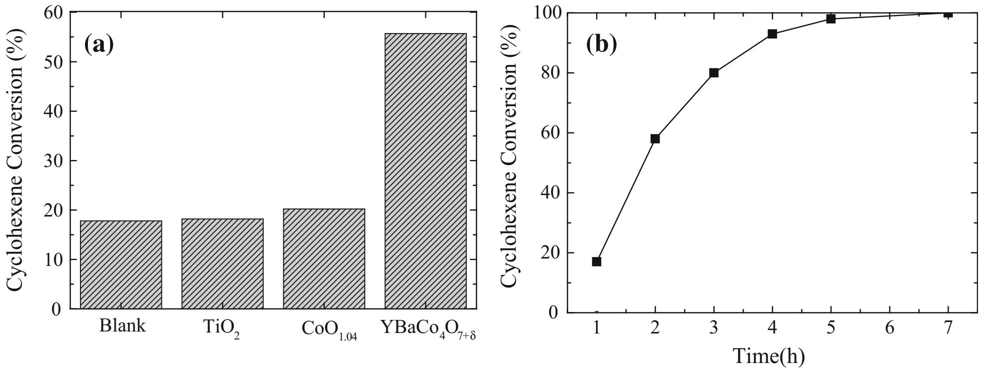

Fig. 5 Cyclohexene conversion **a** for the different catalysts evaluated at 70 °C and after 2-h reaction time, and **b** for the $YBaCo_4O_{7+\delta}$ catalyst with increasing reaction time

Table 2 Enthalpy of immersion for H_2O_2 on the different oxide catalysts evaluated

Sample	$-\Delta H_{imm}$ (J/g)
TiO_2	17
$CoO_{1.04}$	213
$YBaCo_4O_{7.05}$	>3137

calorimetry measurements into H_2O_2 were considered highly useful.

Our immersion calorimetric measurement data summarized in Table 2 show that commercial TiO_2 exhibits a small enthalpy of immersion into H_2O_2, thus suggesting a rather physisorption phenomena without specific liquid–solid interactions. The binary cobalt-oxide powder synthesized as a reference material exhibits a little higher enthalpy of immersion, thus reflecting the presence of specific interactions between H_2O_2 and the Co(II/III) species, in close agreement with the better catalytic behavior of Co versus Ti in oxidation reactions when using H_2O_2 as an oxidant. Most interestingly, for the complex cobalt oxide $YBaCo_4O_{7+\delta}$ the enthalpy of immersion exhibits a dramatic increase above the detection limit of the system. This extremely high enthalpy value clearly reflects the presence of associated reaction processes during the calorimetric analysis. At this point it is also important to mention that hydrogen peroxide decomposition measurements performed outside the calorimetric chamber confirmed the aforementioned findings: whereas the $CoO_{1.04}$ oxide produced essentially no reaction in the presence of hydrogen peroxide, incorporation of a small amount of $YBaCo_4O_{7+\delta}$ resulted in a vigorous exothermic reaction with a large oxygen evolution. After the reaction, the $YBaCo_4O_{7+\delta}$ powder was dried and measured with XRD to verify that it had not decomposed in the process. Moreover, the same catalyst powder sample was also repeatedly made in contact with a fresh batch of H_2O_2 which resulted in a similar formation of gas and heat as in the initial experiment; this confirmed the reusability of $YBaCo_4O_{7+\delta}$ as a catalyst in the oxidation process.

4 Conclusion

We have successfully demonstrated that the complex cobalt oxide, $YBaCo_4O_{7+\delta}$, that is currently strongly emerging as a low-temperature oxygen-storage material works also as an exceptionally efficient catalyst in the oxidation of cyclohexene when hydrogen peroxide is employed as the oxidant. There would be several advantages related with environmental concerns if the commonly used peroxo acid oxidants could be replaced by the green hydrogen peroxide. Our results revealed that compared to e.g. the commercial TiO_2 catalyst, remarkably enhanced catalytic activity was achieved with $YBaCo_4O_{7+\delta}$ for the oxidation process of cyclohexene with H_2O_2. In the 2-h reaction experiments it was three times more active (60 % conversion) than TiO_2 (<20 %), despite its much smaller surface area, and in the longer experiments essentially complete conversion of cyclohexene to reaction products was achieved with a high selectivity to the epoxide. Immersion calorimetry measurements showed that the high catalytic activity may be ascribed to the exceptional ability of $YBaCo_4O_{7+\delta}$ to activate H_2O_2 such that electrophilic oxygen is efficiently released; this active oxygen then provides the excellent oxidation capacity for hydrocarbons.

Most importantly, we foresee that our concept to employ an oxygen-nonstoichiometric redox-active transition-metal oxide as a catalyst in the environmentally benign oxidation reactions of hydrocarbons with hydrogen peroxide should be applicable to a range of nonstoichiometric transition metal oxide materials, thus opening new horizons in the science and technology of catalytic hydrocarbon oxidation processes.

Acknowledgments This work was supported by Academy of Finland (No. 255562) and Generalitat Valenciana (PROMETEO/2009/002).

References

1. Blanco-Brieva G, de Frutos-Escrig MP, Martín H, Campos-Martín JM, Fierro JLG (2012) Catal Today 187:168
2. JJ Spivey (2008) In: B Gerhard (ed) Handbook of heterogeneous catalysis, 2nd edn, vol 5. Wiley-VHC, Weinheim, p. 2394
3. Rudolph J, Reddy KL, Chiang JP, Sharpless KB (1997) J Am Chem Soc 119:6189
4. Murugavel R, Roesky HW (1997) Angew Chem Int Ed 36:477
5. Ivanov S, Boeva R, Tanielyan S (1979) J Catal 56:150
6. Oldroyd RD, Thomas JM, Maschmeyer T, Macfaul PA, Snelgrove DW, Ingold KU, Wayner DDM (1996) Angew Chem Int Ed Engl 35:2787
7. Thomas JM, Raja R (2001) Chem. Commun. 675
8. Boche G, Möbus K, Harms K, Marsch M (1996) J Am Chem Soc 118:2770
9. Shell Oil, GP 1249079, 1971
10. Maschmeyer T, Rey F, Sankar G, Thomas JM (1995) Nature 378:159
11. Corma A, García H (2002) Chem Rev 102:3837
12. Silvestre-Albero A, Grau-Atienza A, Serrano E, García-Martínez J, Silvestre-Albero J (2014) J Catal Commun 44:35
13. Thomas JM, Sankar G (2001) Acc Chem Res 34:571
14. Jinka KM, Sebastian J, Jasra RV (2007) J Mol Catal A 274:33
15. Paterson J, Potter M, Gianotti E, Raja R (2011) Chem Commun 47:517
16. Anand C, Srivinasu P, Mane GP, Talapaneni SN, Benzigar MR, Priya SV, Al-deyab SS, Sugi Y, Vinu A (2013) Microporous Mesoporous Mater 167:146
17. Trovarelli A, de Leitenburg C, Boaro M, Dolcetti G (1999) Catal Today 50:353
18. Reddy SA, Chen CY, Chen CC, Chien SH, Lin CJ, Lin KH, Chen CL, Chang SC (2010) J Mol Catal A 318:60

19. Karppinen M, Yamauchi H, Otani S, Fujita T, Motohashi T, Huang YH, Valkeapää M, Fjellvag H (2006) Chem Mater 18:490
20. Nagai Y, Yamamoto T, Tanaka T, Yoshida S, Nonaka T, Okamoto T, Suda A, Sugiura M (2002) Catal Today 74:225
21. Valldor M, Andersson M (2002) Solid State Sci 4:923
22. Räsänen S, Yamauchi H, Karppinen M (2008) Chem Lett 37:638
23. Kadota S, Karppinen M, Motohashi T, Yamauchi H (2008) Chem Mater 20:6378
24. Motohashi T, Kadota Y, Fjellvåg H, Karppinen M, Yamauchi H (2008) Mater Sci Eng B 148:196
25. Jia Y, Jiang H, Valkeapää M, Yamauchi H, Karppinen M, Kauppinen EI (2009) J Am Chem Soc 131:4880
26. Parkkima O, Yamauchi H, Karppinen M (2013) Chem Mater 25:599
27. Parkkima O, Karppinen M (2014) Eur J Inorg Chem 4056
28. Karppinen M, Matvejeff M, Salomäki K, Yamauchi H (2002) J Mater Chem 12:1761
29. Ha DH, Moreau LM, Honrao S, Henning RG, Robinson RD (2013) J Phys Chem C 177:14303
30. Salek G, Alphonse P, Dulfour P, Guillemet-Fritsch S, Tenauilleau C (2014) Appl Catal B 147:1
31. Biesinger MC, Payne BP, Lau LWM, Gerson A, Smart RStC (2009) Surf Interface Anal 41:324
32. Payne BP, Biesinger MC, McIntyre NS (2011) J Electron Spectrosc Relat Phenom 184:29
33. Biesinger MC, Payne BP, Grosvenor AP, Lau LWM, Gerson AR, Smart RStC (2011) Appl Surf Sci 257:2717
34. Payne BP, Biesinger MC, McIntyre NS (2009) J Electron Spectrosc Relat Phenom 175:55
35. Rajasekar P, Bandyopadhyay SK, Barat P, Sen P, Chakraborty P (1998) Modern Phys Lett B 12:239
36. Barr TL (1991) J Vac Sci Technol A 9:1793
37. Nefedov VI, Gati D, Dzhurinskii BF, Sergushin NP, Salyn YV (1975) Russ J Inorg Chem 20:2307
38. Jung JI, Edwards DD (2011) J Solid State Chem 184:2238
39. Du Y, Kim DJ, Varga T, Wang Z, Szanyi J, Lyubinetsky I (2011) Thin Solid Films 519:5335
40. Qadir MI, Scholten JD, Dupont J (2014) J Mol Catal A Chem 383-384:225
41. Alfayate A, Márquez-Álvarez C, Grande-Casas M, Sánchez-Sánchez M, Pérez-Pariente J (2014) Catal Today 227:57
42. El-Korso S, Khaldi I, Bedrane S, ChoukChou-Braham A, Thibault-Starzyk F, Bachir R (2014) J Mol Catal A Chem 394:89
43. Silvestre-Albero J, Gómez de Salazar C, Sepúlveda-Escribano A, Rodríguez-Reinoso F (2001) Colloids Surf. A 187–188:151
44. Vernimmen J, Guidotti M, Silvestre-Albero J, Jardim EO, Mertens M, Lebedev OI, Van Tendeloo G, Psaro R, Rodríguez-Reinoso F, Meynen V, Cool P (2011) Langmuir 27:3618